CONTINUOUS NANOFIBER YARNS TWISTED THROUGH THREE-DIMENSIONAL HIGH-SPEED SWIRLING AIRFLOW

by

Jian-Xin HE [*a], ***Yu-Man ZHOU*** [a], ***Kun QI*** [a], ***and Fu-Juan LIU*** [b]

[a] College of Textiles, Zhongyuan University of Technology, Zhengzhou, China
[b] College of Textile and Clothing Engineering, Soochow University, Suzhou, China

Review paper
DOI: 10.2298/TSCI1305269H

A new method is proposed to fabricate continuous twisted nanofiber yarns. Nanofibers are bunched by a double conjugate electrospinning, and then twisted through a three-dimensional high-speed swirling airflow. Its principle and process are analyzed theoretically, and the airflow field inside the nozzle chamber is studied numerically, and mechanical properties of nanofiber yarns at different spinning conditions are systematically discussed.

Key words: *nanofiber, yarn, conjugate electrospinning, airflow twisting, numerical simulation*

Introduction

Electrospun nanofibers with nanometric diameter, large specific surface area and small pore size had been found vast potential applications in protective clothing, batteries, biomaterials, tissue scaffolds, nanocomposites, nanocatalysis, sensor, and filtration. However, most of electrospun fibers were produced in the form of randomly oriented non-woven fiber mats. The relatively low mechanical strength and the difficulty in tailoring the fibrous structure had restricted their applications. Hence, there was a considerable interest in the development of continuous yarns made out of nanofibers, which provided an attractive way to incorporate polymeric nanofibers into traditional textiles with broader market.

At present, some methods had been proposed to prepare nanofiber yarns. Electrowet spinning [1] used a coagulating bath to collect nanofibers and draft nanofiber bundles. However, in this way random distribution of nanofibers in the coagulating bath led to bad parallelism in nanofiber bundle. Gu and Shin [2] suggested a method of preparing nanofiber bundles through creating a rotated electric field by an auxiliary electrode. Although this mechanism could form twisted yarns, it could only obtain shorter nanofiber yarns. Dabirian and Hosseini [3] developed a process referred to as conjugated electrospinning to produce continuous yarns from oppositely charged electrospun nanofibers. The nanofiber bundle was aggregated and twisted by rotating unearthed metal disc or funnel placed in the middle of two opposite polarity nozzle. However, all the methods of preparing nanofiber yarns in present studies used twisting ways of mechanical twisting, and the agglomeration, orientation and twisting of nanofiber bundle were occurred at the same time. The way of mechanical twisting led to many problems of yarn hairiness, lower strength and bad yarn evenness due to unoriented nanofibers in the nanofiber bundle. In industrial spinning, yarns were twisted through multi-steps to improve fiber orientation, which, respectively, were separation, orientation, ag-

* Corresponding author; e-mail: hejianxin771117@163.com

glomeration and twisting. Air twisting had significant applications in traditional spinning, such as air-jet spinning [4], air-jet vortex spinning [5], air-textured yarns and so on. Air twisting had many superiorities compared with other twisting ways, including low-costing, high-speed and non-pollution. In addition, it could avoid fiber damage produced by friction between nanofiber and machine.

This paper proposes a new method to prepare continuous nanofiber bundles. Nanofiber bundles were aggregated and orientated by a double conjugated electrospinning and twisted through a 3-D high-speed swirling airflow.

Experimental

Materials

Polyacrylonitrile (PAN, Mw 60,000) and N-N dimethyl formamide (DMF) were supplied by Shanghai Chemical Reagent Co. Ltd., China.

Preparation of spinning solution

PAN solution of 15 wt.% concentration was prepared through dissolving PAN powder in DMF solution at 80 ºC for 3 hours.

Experimental of spinning continuous nanofiber yarn

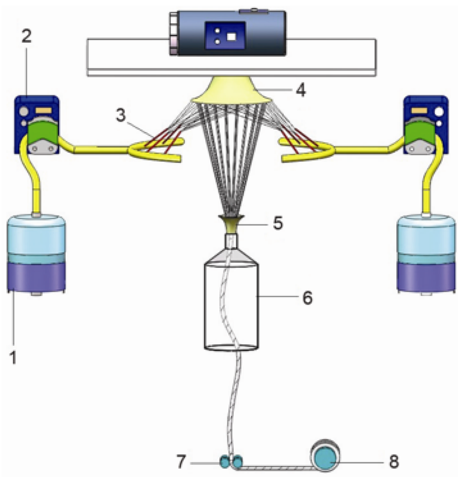

Figure 1. The set-up of nanofiber air-jet spinning; *1 – fluid reservoir, 2 – metering pump, 3 – nozzle, 4 – metal funnel, 5 – buncher, 6 – nozzle twisting device, 7 – guide roller, 8 – winder device*

The set-up of nanofiber air-jet spinning is shown in fig. 1, including fluid reservoirs, metering pump, nozzles, metal funnel, buncher, nozzle twisting device, guide roller, and winder device. A couple of liquid transport tubes equipped with two nozzles, which connected separately with the positive and negative electrodes of the DC power supply, arranged symmetrically on both sides under funnel collector. The funnel collector was not earthed and the buncher connected with nozzle twisting device.

The schematic diagram of nozzle twisting device is shown in fig. 2, consisting of two air vessels, four jet orifices and a twisting chamber with a yarn passage through it. Twisting chamber is composed of three parts, including a small cylindrical tube at the top, a laddertron in the middle and a cylindrical tube with bigger diameter at the bottom. Compressed air was ejected into the twisting chamber with high speed from four jet orifices that were tangential to the nozzle wall. High-speed 3-D swirling airflow formed in twisting chamber was used to twist nanofiber bundle.

PAN solution was transported to nozzles with uniform rates through metering pump. Nanofibers electrospun from the oppositely charged nozzles were deposited onto the rotary funnel to form a nanofiber web. By the drawing of an insulating rod, the nanofiber web was pulled into fiber bundle. Then the fiber bundle was transported into buncher. Due to the adsorption of negative pressure, nanofiber bundle was sucked into nozzle chamber and then twisted. Finally twisted nanofiber yarn was winded to winder device.

A voltage of 20 kV was applied to the nozzles with the distance between homopolar nozzles at 5.5 cm. The distance from positive nozzles to negative nozzles was 18 cm. The overall flow rate of spinning solution was 6.4 ml/h and the flow ratio of positive and negative nozzle was 5/3. The pressure of jet orifice was at the range from $3\cdot10^5$ Pa to $5\cdot10^5$ Pa. The take-up speed of winder device was 30 rpm.

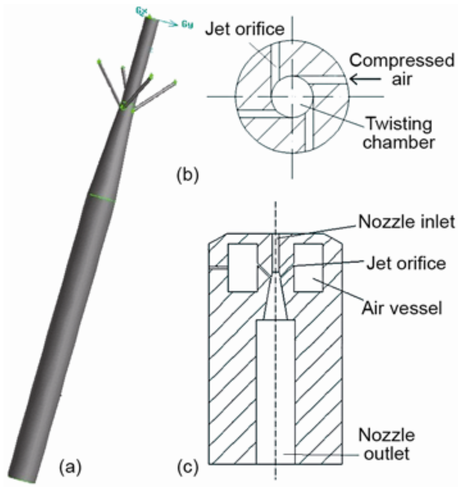

Figure 2. The schematic diagram of nozzle twisting device; (a) 3-D model, (b) cross--section, (c) lengthwise section

Characterizations

The nanofiber yarns were coated with gold film in order to observe fiber and yarn morphologies. The instrument was a JEOL JSM-5600LV electron microscopic with an accelerating voltage of 10 kV.

The tensile properties were measured with an INSTRON 365 tester at room temperature under room humidity. The gauge length was set to be 15 cm and the rate of the crosshead was 150 mm/min. The reported data of breaking strength and elongation represent the average results of 20 tests.

Results and discussion

The electric field simulation and preparation of nanofiber bundles

Figure 3 shows the electric field distribution of double conjugate electrospinning simulated by Ansoft Maxwell12.0 software, in which two pairs of nozzles were positively and negatively charged, respectively, and the funnel collector was not earthed. The distribution of equipotential lines was shown in fig. 3(a), in which re-

(a)
(b)
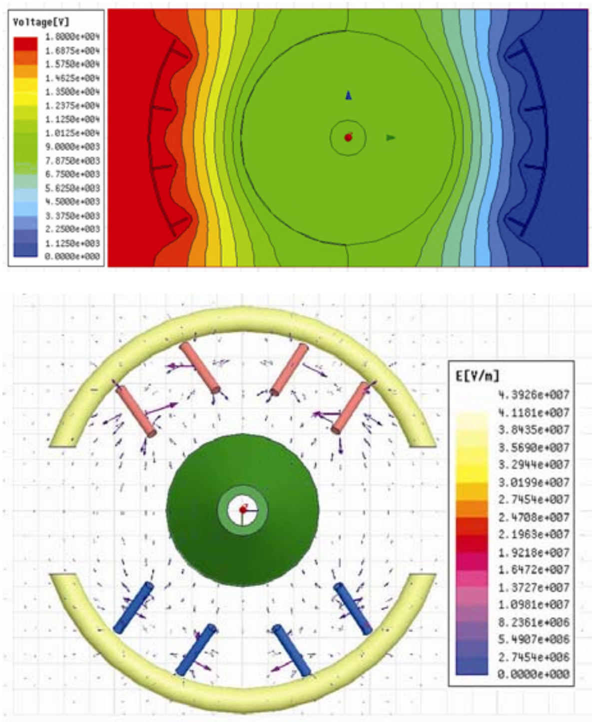

Figure 3. The electric field simulation of double conjugate electrospinning; (a) the distribution of equipotential lines, (b) the distribution of 3-D electric intensity vector
(for color image see journal web site)

gions with different colors indicated different voltage. The voltage of bottle green and mazarine regions was 0 V. When the color indicating voltage in the region from positive nozzles to the side of the funnel mouth changed from red to yellow and then to green, it meant the voltage of positive nozzle decreased from 8000e+004 V to 0 V. However, the voltage of negative nozzle increased from 0 V to 8750e+003 V when the color in the region from negative nozzles to the side of the funnel mouth changed from mazarine to light blue and then to green. The distribution of 3-D electric intensity vector was shown in fig. 3(b), in which arrow denoted the direction and intensity of electric field. The bigger red arrows indicate that electric intensity was stronger. Not only the region between positive and negative nozzles existed electric field due to the electrostatic induction, but the region from the tip of the nozzle to the side of the funnel mouth existed electric field. Meanwhile, charges carried by positive and negative nozzles were neutralized at the funnel. In addition, it was necessary to adjust the distance among nozzles properly because of repellant of homopolar nozzles.

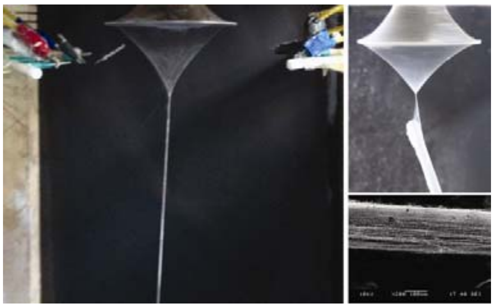

Figure 4. The process of preparing continuous nanofiber bundle

The charged jets ejected from two pairs of oppositely charged nozzles would be attracted towards the side of the inductive funnel with opposite charges owing to existing induction fields between both edges of the funnel and their nearby charged nozzles. Then the jets got neutralized and formed a hollow nanofiber web with its edges connecting to the funnel end. After drawn by an insulating rod placed near the central area of the funnel, the hollow nanofiber web formed a "fibrous cone" with its apex attaching to the rod. Further drawing the cone apex induced the formation of orientated nanofiber bundle (fig. 4). Finally the nanofiber bundle was transported into buncher. Uncharged nanofiber bundle could be drawn stably because the charged jets ejected from two pairs of oppositely charged nozzles get neutralized.

Numerical simulation of airflow in the nozzle twisting device

Compressed air was ejected into the twisting chamber through four narrow jet orifices with tangential direction. The flow model of airflow in nozzle twisting device was 3-D, compressible, steady, viscous turbulent flow of a perfect gas in view of higher Reynolds number and compressibility of the airflow [6]. Mass conservation equation, momentum conservation equation, energy conservation equation and the equation of state could be written as:

$$\mathrm{div}(\rho\vec{v}) = 0 \tag{1}$$

$$\mathrm{div}(\rho v\vec{v} - \tau) = -\mathrm{grad}p + \mathrm{f} \tag{2}$$

$$\mathrm{div}\left(\rho\vec{v}T\right) = \mathrm{div}\left(\frac{k}{c_p}\mathrm{grad}T\right) + S_T \tag{3}$$

$$p = \rho \mathrm{R} T \tag{4}$$

where ρ, p, f, T, $\vec{v}$, k, τ, and S_T are the air density, pressure, gravity, temperature, velocity vector, specific heat capacity, viscous stress tensor, and viscosity dissipation rate, respectively. R is the gas constant.

The standard k-ε turbulence model was set based on the consideration of turbulent flow of the fluid, applicability, accuracy, and simplicity [7]. An unstructured mesh was used to mesh the entire region and the structure of the nozzle twisting device was simplified in order to reduce meshing time. Pressure inlet condition was used at the jet orifices inlet and pressure outlet condition was used at nozzle chamber inlet and outlet. Non-slip boundary condition was applied at wall.

Flow characteristic of the airflow in nozzle twisting device

The results of numerical simulation on the flow characteristics of airflow in the nozzle twisting device were analyzed with the jet orifices pressure at $5\cdot10^5$ Pa. Figure 5 shows streamlines in nozzle twisting device. Regular swirling airflow was formed when compressed air was ejected into the twisting chamber with tangential direction from jet orifices, fig. 5(a). The streamlines of airflow in the whole flow field is shown in fig. 5(b). Airflow flowed from nozzle inlet joined into the airflow ejected from jet orifices and then formed complex movement locus due to the combined action of the two airflow. The airflow had a larger swirl near the outside of the twisting chamber and the movement locus was regular. However, the airflow had a small swirl near the axis of the twisting chamber and the movement locus of the airflow was more complicated in the middle region.

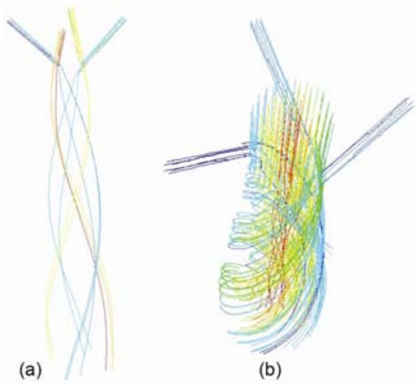

Figure 5. Streamlines in nozzle twisting device; (a) streamlines starting from jet orifice, (b) streamlines starting from jet orifice and nozzle inlet
(for color image see journal web site)

Figure 6 represents the velocity vector plot in the whole computational domain of the nozzle twisting device. The velocity reached the highest value at the jet orifice outlet and then decreased rapidly after the air flows into the laddertron. The velocity of airflow had the minimum value at nozzle outlet. In order to get a clear view of the flow characteristics inside the twisting chamber, the velocity vectors in different plane are shown in fig. 7. Velocity vectors at vertical section of $X = 0$ mm are shown in fig. 7(a). From fig. 7(a) it is obvious that the direction of airflow was changed below the laddertron. A weaker airflow flowed into the twisting chamber from nozzle outlet and moved upstream along the wall of the twisting chamber. Then it collided with the airflow ejected from jet orifices. The velocity of airflow decreased sharply and changed its direction after the collision. Finally the core of swirling airflow was diverged the axis of the twisting chamber, figs. 7(c) and 7(d). Figure 7(b) is the velocity vectors plot in the plane of $Z = 4$ mm at the position of jet orifice outlet. Airflow had a sudden expansion and drove the movement of the air in twisting chamber, then formed high-speed swirling airflow after compressed air was jetted into the twisting chamber through the jet orifice with tangential direction. The movement of the airflow could be divided into two regions, which are high-speed swirling airflow around outer region and low-speed airflow around axis. Figures 7(c) and 7(d) are the cross-section of $Z = 8$ mm and $Z = 13$ mm, which were located at the middle of laddertron and the interface between laddertron and nozzle outlet, respectively. When the high-speed swirled airflow moved to downstream, the airflow took the regular swirling movement and the value of velocity decreased obviously.

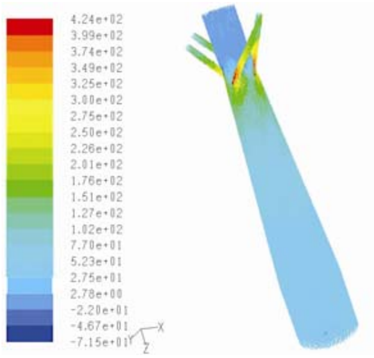

Figure 6. Velocity vectors plot of the airflow in nozzle twisting device

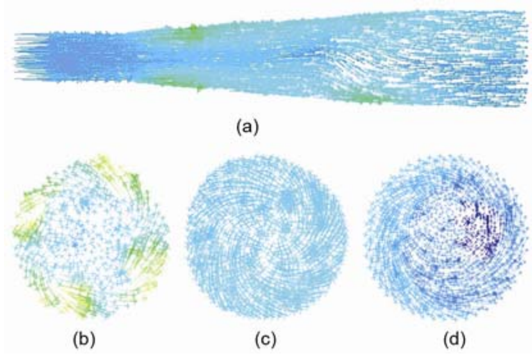

Figure 7. Velocity vectors plot of the airflow at different section; (a) X = 0 mm, (b) Z = 4 mm, (c) Z = 8 mm, and (d) Z = 13 mm

Static pressure distribution of the airflow in nozzle twisting device

Static pressure distribution of the airflow in nozzle twisting device is shown in fig. 8(a). The value of static pressure in most areas was negative and the pressure distribution inside the nozzle twisting device was axial symmetric. The pressure reached the highest value at the jet orifice inlet and decreased the minimum at the jet orifice outlet. The value of pressure in twisting chamber was at the range from $0.6 \cdot 10^5$ Pa to $1.0 \cdot 10^5$ Pa. The distribution of the pressure could divide into two regions, fig. 8(b). Some reverse flow along the wall of twisting chamber led to higher static pressure near the wall. External air entered into twisting chamber and got a certain speed because the internal pressure was lower than the external atmosphere pressure. Nanofiber bundle was sucked into nozzle inlet with the function of the suction airflow. In the process of spinning, nanofiber bundle was twisted by the high-speed swirling airflow ejected from jet orifices, and twisted nanofiber yarn obtained certain strength to meet the requirement of subsequent working procedure.

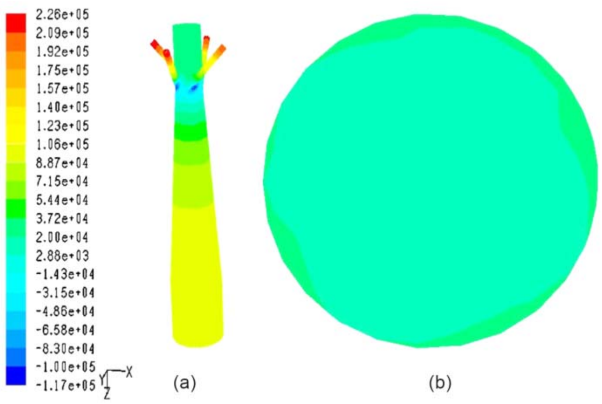

Figure 8. Static pressure distribution of *(a) the airflow in the whole computational domain, and (b) the airflow at cross section of Z = 4 mm*

Velocity distribution of the airflow in nozzle twisting device at different pressure

The structure and property of twisted nanofiber yarn depended on the velocity distribution of the airflow inside the nozzle twisting device. With a view to the characteristic of nanofiber yarn, this paper discussed three different parameters, $3 \cdot 10^5$ Pa, $4 \cdot 10^5$ Pa and $5 \cdot 10^5$ Pa, respectively. The simulated results of tangential velocity distribution along radial position for the plane of $Z = 4$ mm was shown in fig. 9(a). The tangential velocity increased with the increasing of jet orifice pressure from $3\cdot10^5$ Pa to $5\cdot10^5$ Pa. However, the distribution rule did not change and the curves exhibited some axisymmetric nature. The tangential velocity had a small value extending to the nozzle axis, then a steep increase in the curves could be observed on both sides and the value rapidly decreased to zero near the wall. The distribution rule of the tangential velocity inside the nozzle twisting device indicated that the distribution of the airflow presented a typical characteristic of swirling airflow [8]. This agreed with the earlier research on an air vortex [9]. The separated ends of the fibers rotated tangentially with the action of the swirling airflow and helically wrapped onto the main body of the strand to form the yarn when twisting yarns due to the high tangential velocity.

Figure 9(b) shows the radial velocity distribution along radial position for the plane of $Z = 4$ mm. Being different from the tangential velocity, the value of radial velocity was lower. The value of radial velocity reached the highest near the wall. The movement of the fibers could be affect by the radial velocity of the airflow. Nanofibers moved to outside easily and the separation of the fiber would be enhanced when the radial velocity was higher. More nanofibers could be separated at the jet orifice pressure of $5\cdot10^5$ Pa compared to the other two conditions.

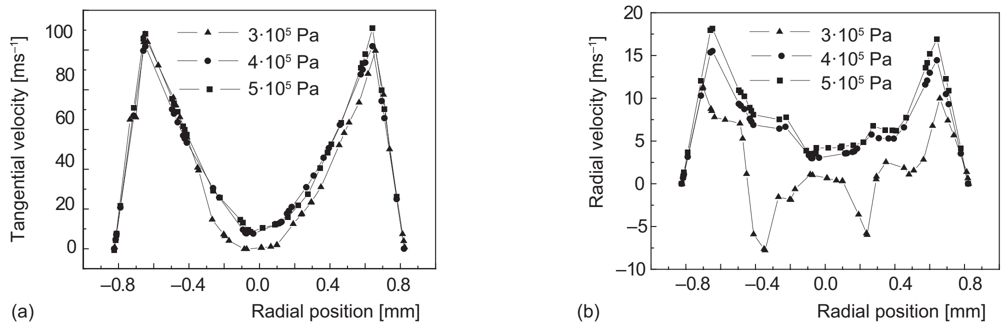

Figure 9. (a) Tangential velocity distribution, (b) Radial velocity distribution of the airflow along radial position

The twisting and property of the nanofiber yarn

The variation of airflow velocity in nozzle twisting device depended on jet orifice pressure. Airflow had different tangential velocity when given different pressure. The tangential velocity increased with the increasing of pressure, and the twisting level of yarn increased. The twisting angle of yarn could reach the highest value of 39.1° at the jet orifice pressure of $5\cdot10^5$ Pa (fig. 10).

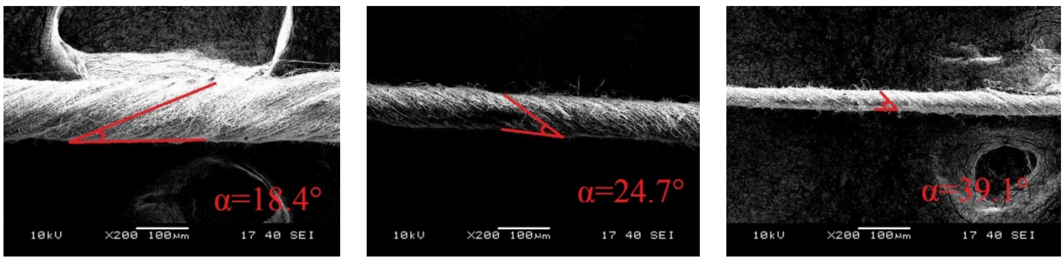

Figure 10. The electron microscope image of different jet orifice pressure on nanofiber yarn; (a) $3\cdot10^5$ Pa, (b) $4\cdot10^5$ Pa, (c) $5\cdot10^5$ Pa

The mechanical property of yarn depended on the twisting level. When increasing jet orifice pressure, the twisting level of yarn increased. In addition, the cohesive force and frictional resistance among fibers increased. When the jet orifice pressure increased from $3 \cdot 10^5$ Pa to $5 \cdot 10^5$ Pa, the strength at breaking increased from 18.83 to 55.69 MPa and elongation at breaking increased from 25.46% to 41.31%, respectively.

Conclusions

Continuously twisted nanofiber yarns were prepared by the combinations with conjugate electrospinning and airflow twisting. Airflow flowed from nozzle inlet joined into the airflow ejected from jet orifices and then formed complex movement locus.

The airflow velocity reached the highest value at the jet orifice outlet and then decreased rapidly after the air flowed into the laddertron. The velocity of airflow had the minimum value at nozzle outlet. The value of static pressure in most areas was negative and the pressure distribution inside the nozzle twisting device was axial symmetric. The pressure had the highest value at the jet orifice inlet and decreased to the minimum at the jet orifice outlet. Twisting level, strength and elongation at breaking of the nanofiber yarn increased with the increasing of pressure from $3 \cdot 10^5$ Pa to $5 \cdot 10^5$ Pa, and the twisting angle of nanofiber yarn reached the highest value of 39.1° when jet orifice pressure at $5 \cdot 10^5$ Pa.

Acknowledgments

This work was supported by National Natural Science Foundation of China (No. 51203196), and the United Foundation from National Natural Science Foundation of China and The People's Government of Henan Province for Cultivating Talents (No. U1204510), and the Natural Science Foundation of Henan Province, China (No. 122300410242) is gratefully acknowledged.

References

[1] Smit, E., Buttner, U., Continuous Yarns from Electrospun Fibers, *Polymer, 46* (2005), 8, pp. 2419-2423
[2] Gu, B. K., Shin, M. K., Direct Fabrication of Twisted Nanofibers by Electrospinning, *Applied Physics Letters, 90* (2007), 26, pp. 263902-263903
[3] Dabirian, F., Hosseini, Y., Manipulation of the Electric Field of Electrospinning System to Produce Polyacrylonitrile Nanofiber Yarn, *Journal of the Textile Institute, 98* (2007), 3, pp. 237-241
[4] Basal, G., Oxenham, W., Vortex Spun Yarn *vs.* Air-Jet Spun Yarn, *Autex Research Journal, 3* (2003), 3, pp. 96-101
[5] Basal, G., Oxenham, W., Effects of Some Process Parameters on the Structure and Properties of Vortex Spun Yarn, *Textile Research Journal, 76* (2006), 6, pp. 492-499
[6] Bakic, V., Zivkovic, G., Numerical Simulation of the Air Flow around the Arrays of Solar Collectors, *Thermal Science, 15* (2011), 2, pp. 457-465
[7] Moldovanu, D., Burnete N., Computational Fluid Dynamics Simulation of a Single Cylinder Research Engine Working with Biodiesel, *Thermal Science, 17* (2013), 1, pp. 195-203
[8] Chang, F., Dhir, V. K., Turbulent Flow Field in Tangentially Injected Swirl Flows in Tubes, *International Journal of Heat and Fluid Flow, 15* (1994), 5, pp. 346-356
[9] Zhang, W. G., *The Problem of Air Flow in Textiles,* Textile Industry, Beijing, China, 1989

Paper submitted: January 28, 2013
Paper revised: April 28, 2013
Paper accepted: May 14, 2013